

**Apoptotic cells ameliorate chronic intestinal inflammation by enhancing
regulatory B cell function**

Md. Mesbah Uddin Ansary¹, Shunji Ishihara¹, Akihiko Oka¹, Ryusaku Kusunoki¹,
Naoki Oshima¹, Takafumi Yuki², Kousaku Kawashima¹, Hidetaka Maegawa³, Nobuhito
Kashiwagi³, Yoshikazu Kinoshita¹

¹Department of Internal Medicine II, Shimane University School of Medicine, Japan

²Department of Gastrointestinal Endoscopy, Shimane University Hospital, Japan

³JIMRO Co., Ltd

Short title: Apoptotic cells and intestinal inflammation

Key words: apoptotic cells, regulatory B cells, IL-10, phagocytosis, inflammatory
bowel disease

Address for correspondence and reprint requests to:

Shunji Ishihara, MD, PhD

Department of Internal Medicine II

Shimane University, Faculty of Medicine

89-1, Enya-cho, Izumo, Shimane, Japan

Tel: +81-853-20-2190

Fax: +81-853-20-2187

E-mail: si360405@med.shimane-u.ac.jp

Conflicts of interest:

This work was supported in part by JIMRO Co., Ltd in Japan.

Abstract

Apoptosis is a programmed physiological death of unwanted cells, and handling of apoptotic cells (ACs) is thought to have profound effects on immune-mediated disorders. However, there is scant information regarding the role of ACs in intestinal inflammation, in which immune homeostasis is a major concern. To investigate this, we injected ACs into an SCID adoptive transfer model of chronic colitis in the presence and absence of co-transferred whole B or regulatory B cell (Breg)-depleted B cells. We also injected syngeneic ACs into AKR/N mice as a control and into milk fat globule-epidermal growth factor 8 knockout (MFG-E8 KO) mice deficient of phagocytic function. Chronic colitis severity was significantly reduced in the AC as opposed to the PBS group with co-transferred whole B cells. The AC-mediated effect was lost in the absence of B cells or presence of Breg-depleted B cells. In addition, ACs induced splenic B cells to secrete significantly increased levels of IL-10 in AKR/N mice but not MFG-E8 KO mice. Apoptotic leukocytes were induced by reactive oxygen species (ROS) during granulocyte/monocyte apheresis (GMA) therapy in rabbits and H₂O₂-induced apoptotic neutrophils ameliorated mice colitis. Our results indicate that ACs are protective only in the presence of B cells and phagocytosis of ACs induced IL-10 producing Bregs. Thus, the ameliorative effect seen in this study might have been exerted by AC-induced Bregs via increased production of the immunosuppressive cytokine IL-10, while an AC-mediated effect may contribute to the anti-inflammatory effect of GMA as a novel therapeutic mechanism for IBD.

Introduction

Apoptotic cell (AC) death is a highly controlled means of eliminating dangerous, damaged, or unnecessary cells without causing an inflammatory response or tissue damage (1, 2). In recent years, a number of studies have demonstrated that ACs are not inert and can significantly influence the immune system (3, 4), as exposure to ACs can induce suppression of immunity through engulfment of dead cells by dendritic cells (5-7). On the other hand, decreased phagocytosis of ACs contributes significantly to the development of systemic lupus erythematosus (SLE) in mice and humans (8). Thus, immune response to ACs is largely dependent on the capability of handling these cells by the host immune system.

AC-dependent immunosuppression is generated by several mechanisms including production of immunosuppressive cytokines by phagocytes (9), deletion of T cells (10), induction of regulatory B cells (Bregs) (11), and activation of CD8⁺ regulatory T cells (Tregs) (5). ACs were shown to protect mice from autoimmune-mediated inflammation (12, 13) and induce B cells to adopt an IL-10-secreting Breg phenotype (11). TGF- β and IL-10 are the most notable cytokines among the several soluble effectors reported to be involved in immunosuppression by ACs (9, 14). Despite these findings, the key cellular and molecular mechanisms that promote tolerance have yet to be characterized.

Ulcerative colitis (UC) and Crohn's disease (CD), two major forms of human inflammatory bowel disease (IBD), are characterized by chronic immune-mediated disorders and affected individuals experience relapsing episodes of abdominal pain, diarrhea, melena, and weight loss (15). Although there is increasing evidence that genetic, immunological, and environmental factors may be involved in the pathogenesis

of IBD, their details remain unclear (16-20). Current treatment regimens for IBD are based on suppression and control of inflammation using corticosteroids, immune-modulating drugs, and anti-TNF antibodies (21). Although such drug therapies targeting inhibition of the inflammatory process may provide better therapeutic options for IBD, numerous studies have been conducted to evaluate innovative approaches. Recently, we reported anti-inflammatory roles of Breg in a mouse colitis model (22), which might lead to a novel therapeutic strategy for IBD. However, methodologies regarding the effective activation or induction of Bregs *in vivo* remain unknown. Since previous studies revealed the immunosuppressive effects of ACs associated with the function of Bregs, we speculated that ACs may ameliorate intestinal inflammation by controlling that function.

In the present study, we initially investigated the immunosuppressive potential of injected apoptotic thymocytes in a colitis model of SCID mice by adoptive transfer of CD4⁺ T cells co-transferred with whole or Breg-depleted B cells. Next, we employed milk fat globule epidermal growth factor (EGF) factor 8 knockout (MFG-E8 KO) mice with impaired uptake of ACs (23) and examined whether engulfment of injected ACs regulates the function of Bregs in the anti-inflammatory process. Evaluation of colitis parameters indicated that AC-mediated immunosuppressive effects were generated by induction of an IL-10-producing Breg population, which was dependent on phagocytosis of ACs in the mouse spleen. Finally, we found that apoptosis was induced among circulating leukocytes by granulocyte/monocyte apheresis (GMA) therapy using Adacolumn and confirmed experimentally that this apoptosis-inducing feature might contribute to the anti-inflammatory effects of GMA as a novel therapeutic mechanism for IBD.

Materials and methods

Reagents

We used the following antibodies (Abs) for flow cytometry: PE-conjugated anti-mouse CD19 (BD Biosciences-Pharmingen, San Diego, CA, USA), FITC-conjugated anti-mouse CD1d (BD Biosciences-Pharmingen), APC-conjugated anti-mouse CD19 (BD Biosciences-Pharmingen), PE-conjugated anti-mouse IL-10 (BD Biosciences-Pharmingen), and PE conjugated anti-mouse CD62L (L-selectin) monoclonal antibody (Beckman Coulter Brea, CA). We also utilized anti-mouse CD4 and CD19 microbeads (Miltenyi Biotec). For intracellular examinations, GolgiStop (BD Biosciences-Pharmingen) was used. Phorbol 12-myristate 13-acetate (PMA) and ionomycin were obtained from Sigma-Aldrich. Unmethylated CpG DNA (5'-TGACTGTGAACGTTTCGAGATGA-3') was synthesized by Hokkaido System Science Co., Ltd.. Enzyme immunoassays (EIA) kits for Mouse IL-10 Immunoassays were obtained from R&D Systems.

Flow cytometry

The above mouse Abs were used for flow cytometry analyses as necessary. GolgiStop was added to the medium during the last 5 hours of the culture period for intracellular cytokine staining. Flow cytometry analysis was performed using an FACS Aria II (BD Biosciences-Pharmingen), FACSCalibur (BD Biosciences-Pharmingen), or FACSCan (BD Biosciences-Pharmingen).

Mice

SAMP1/Yit (SAMP1) mice were kindly provided by S. Matsumoto (Yakult Central

Institute for Microbiological Research, Tokyo, Japan). AKR/N (AKR) mice were purchased from Japan SLC, Inc. (Hamamatsu, Japan). AKR mice share a genetic background with SAMP1 mice and their entire MHC region is identical. SCID mice (CB17/Icr-Prkdc^{scid}/CrICrlj) were purchased from Charles River Japan, Inc. (Kanagawa, Japan). C57BL/6N mice were purchased from Japan SLC, Inc. (Hamamatsu, Japan). Mfge8^{-/-} mice with a C57BL/6 genetic background were obtained from RIKEN BRC. All experiments with animals in this study were approved by the Ethics Committees for Animal Experimentation of Shimane University and JIMRO Co., Ltd, and they were handled according to institutional guidelines.

Generation of apoptotic thymocytes

Thymi were removed from 4-week-old AKR mice and teased into single-cell suspensions. They were then cultured at a concentration of 10⁷ cells/ml in RPMI 1640 medium supplemented with 10% heat-inactivated FBS, 10 mM HEPES, 100 U/ml penicillin (Invitrogen), 100 µg/ml streptomycin (Invitrogen), and 10 µM dexamethasone (Sigma-Aldrich; Japan) for 8 hours at 37°C with 5% CO₂. Apoptotic cell death stage was analyzed using a PE Annexin V apoptosis detection kit I (BD Biosciences-Pharmingen) with a FACSCalibur (BD Biosciences-Pharmingen). After extensive washing, these apoptotic thymocytes were injected in an intravenous (i.v.) manner for *in vivo* experiments.

Induction of chronic colitis in SCID mice and apoptotic cell co-injection

For this experiment, we used SAMP1 CD4⁺ MLN T cell-mediated chronic colitis model SCID mice previously reported by our group (22). CD4⁺ T cells were magnetically

isolated from mesenteric lymph nodes (MLNs) of SAMP1 mice (30-50 weeks old) by positive selection with CD4 microbeads. Isolated CD4⁺ T cells (5×10^5 cells/mouse) were intraperitoneally injected into SCID mice (8-10 weeks old) (day 1) to induce chronic colitis after 6-7 weeks. To investigate the protective effects of ACs, dexamethasone induced apoptotic thymocytes (1×10^7 cells/mouse) or PBS (vehicle) were co-transferred i.v. (tail vein) (week 1) into the SAMP1 CD4⁺ MLN T cell-mediated chronic colitis mouse model.

Sorting of B cells and co-transfer experiments

We recently reported that CD19^{hi}CD1d^{hi} cells, which secrete high levels of IL-10 (22), can be considered as a Breg-rich population. Total splenic CD19⁺ B cells were magnetically isolated from AKR mice (15-25 weeks old) by positive selection with CD19 microbeads. CD19^{hi}CD1d^{hi}-depleted B cells, excluding the Breg population, were sorted from whole splenic CD19⁺ B cells using an FACS sorting system. To investigate the effects of AC-Bregs interaction in chronic intestinal inflammation, whole or CD19^{hi}CD1d^{hi}-depleted B cells (2×10^6 cells/mouse) were co-transferred i.v. (tail vein) (day 0) into the above T cell-mediated chronic colitis model, followed by i.v. injection of ACs (at week 1). Body weight (BW) changes were monitored weekly using a top loading balance. All mice were euthanized at 7 weeks after colitis induction, and the severity of colitis was examined using the disease activity parameters BW and histological score. The expression levels of macrophage inflammatory protein (MIP)-2 and IL-1 β in intestinal tissues were determined using real-time PCR.

ELISA

Concentrations of murine IL-10 were measured in cell culture supernatants using a specific ELISA kit, according to the manufacturer's instructions.

Histological examinations

Tissues taken from the distal part of the colon were formalin-fixed and embedded in paraffin blocks. For histological examinations, 3- μ m paraffin sections were stained with hematoxylin and eosin to visualize their general morphology under a light microscope. Histological grading was evaluated as previously described (24).

RNA extraction and real-time PCR

Total RNA was extracted from each sample using an RNeasy Protect Mini Kit (Qiagen Inc., Tokyo, Japan), then equal amounts of RNA were reverse transcribed into cDNA using a QPCR cDNA Kit (Stratagene, La Jolla, CA, USA). All primers (see Table S1, Supplemental Digital Content 1, for the primer sequences) used were flanked by intron-exon junctions using the NCBI blast tool and Primer3 software. Quantitative real-time PCR was performed using a StepOnePlus Real Time PCR System (Applied Biosystems, Foster City, CA, USA) with SYBR Green PCR master mix (Applied Biosystems), according to the manufacturer's instructions. The levels of mRNA were normalized to that of β -actin using sequence detector software (Applied Biosystems).

Antigen-induced arthritis in rabbits

Arthritis was induced by injection of ovalbumin (OVA: Sigma-Aldrich, Saint Louis, MO) into joints of OVA-immunized rabbits according to the method of Pettipher *et al.* (25). Briefly, Japanese white rabbits (kb1) weighing approximately 3 kg (Kitayama

LABES, Nagano, Japan) were immunized by intra-dermal injection of 4 mg OVA in 1 ml of Freund's complete adjuvant (Gibco, Paisley, Scotland). The animals were re-immunized 14 days later in the same manner. Five days after the second immunization, arthritis was induced in a knee joint by intraarticular injection of 5 mg OVA in 1 ml of sterile saline, while the contralateral knee joint was injected with 1 ml sterile saline to serve as a within animal control.

GMA for rabbit arthritis model

GMA for rabbit arthritis model was established as reported by Kashiwagi *et al.* (26). We used a mini GMA column with a diameter of 1.5 cm and length of 10 cm, which contained 11 g of cellulose diacetate carriers (G-1 beads) developed by JIMRO Co., Ltd (Takasaki, Japan) for the Adacolumn™. The G-1 beads have a diameter of approximately 2 mm. Apheresis was performed at a flow rate of 1.5 ml/minute for 60 minutes. Small size columns with a volume equal to the priming volume of the GMA column but without carriers were used as sham columns (Fig. 5A). It has been shown that immunoglobulin and complement fragments such as C3bi deposit onto G-1 beads during apheresis, and then granulocytes and monocytes are selectively adsorbed to the beads by using their Fc receptor and complement receptor (27).

Detection of superoxide generation by leukocytes in GMA column

Superoxide generation in the GMA column was detected according to the method of Nakano *et al.* (28). Briefly, each rabbit was continuously infused with 185 μ M of a lucigenin derivative of Cypridinacea (MCLA) at a flow rate of 10 ml/hour starting 10 minutes prior to initiation of GMA. The GMA column was placed inside the chamber of

a photon counting unit shielded from light, then GMA was performed. The amount of O_2^- (superoxide anion radical) was measured by directly counting the number of photons emitted by MCLA upon reaction with O_2^- .

Measurement of apoptotic neutrophils from rabbit peripheral blood

Blood was collected using acid-citrate-dextrose as an anticoagulant to minimize neutrophil activation and maintain stability. Neutrophils were isolated using discontinuous Percoll gradients (Pharmacia Fine Chemicals, Piscataway, NJ) (65% and 70% in diluted PBS) by slight modification of a method previously described (29). Isolated neutrophils at 1×10^6 cells/ml in RPMI-1640 medium supplemented with 10% FBS were incubated at 37°C in a CO₂ incubator for 18 hours. Apoptosis of neutrophils was assessed using a previously published procedure (30). Briefly, cultured neutrophils at 1×10^6 cells/ml were washed with PBS and fixed for 30 minutes in ice-cold 70% ethanol. Fixed cells were then washed twice with cold PBS and resuspended in 500 μ l of PBS containing 250 μ g/ml RNase and 5 μ g/ml of propidium iodide. The suspension was incubated in the dark at room temperature for 15 minutes before analysis with a FACScan (BD Bioscience). The proportion of cells within the hypodiploid peak has been shown to correlate with apoptosis (30).

Peritoneal exudate cells isolation and apoptosis induction by hydrogen peroxide

Peritoneal exudate cells (PECs), containing 65% to 85% neutrophils (31), were isolated using a previously described method with minor modifications (31, 32). Mice were injected intraperitoneally with 1 ml of 2% sodium caseinate (Wako Pure Chemical Industries, Osaka, Japan) in PBS. Twenty hours later, PECs were collected by lavage of

the peritoneum of each mouse with Hank's Balanced Salt Solution (HBSS) in a total volume of 8 ml containing 1 U/ml heparin. The PECs were then incubated at a concentration of 2×10^6 cells/ml in RPMI 1640 medium supplemented with 100 U/ml penicillin (Invitrogen), 100 µg/ml streptomycin (Invitrogen), and 500 µM H₂O₂ (Sigma-Aldrich) for 1 hour at 37°C with 5% CO₂. Apoptotic cell death stage was analyzed using a PE Annexin V apoptosis detection kit I (BD Biosciences-Pharmingen) with a FACSCalibur (BD Biosciences-Pharmingen). After extensive washing, these apoptotic PECs (APECs) were injected i.v. for *in vivo* experiments.

Flow cytometric analysis of L-selectin expression on neutrophils

Rabbit model. First, 200 µl of an EDTA-blood sample was labelled with FITC conjugated anti-L-selectin monoclonal antibody (LAM1-3; Coulter Healeah, FL) for 30 minutes at 4°C, then incubated blood cells were treated with 2 ml of FACS lysing solution (Becton Dickinson, San Jose, CA) for 10 minutes at room temperature. After washing twice with PBS containing 0.1% NaN₃, 500 µl of 1% paraformaldehyde in PBS was added and subjected to flow cytometry. Neutrophils were discerned by a combination of low angle forward scattered and right angle scattered laser light, and more than 5000 events were acquired in the gate.

Mouse model: First, 5×10^5 of live or apoptotic PECs from an AKR mouse were labelled with PE conjugated anti-CD62L monoclonal antibody (Beckman Coulter Brea, CA) for 30 minutes at 4°C. After washing twice with PBS, 500 µl of PBS was added and the samples were subjected to flow cytometry.

Statistical analysis

All results are expressed as the mean with the standard error of the mean (SEM) or as a range, as appropriate. Student's *t*, Mann-Whitney, and Wilcoxon-signed-rank tests were used as appropriate to examine significant differences. *P* values less than 0.05 were considered to be significant. All statistical analyses were performed using statistical analysis software (SPSS, version 12.0 for the PC; SPSS Japan Inc.).

RESULTS

ACs do not ameliorate chronic colitis in SCID mice in absence of mature B cells

Adoptive transfer of CD4⁺ T cells isolated from the MLNs of SAMP1 mice induced remarkable intestinal inflammation in mature B- and T cell-negative SCID mice (22). To investigate the effects of ACs on intestinal inflammation, we used a SAMP1 CD4⁺ MLN T cell-induced chronic colitis model of SCID mice. Dexamethasone (Dex)-induced apoptotic thymocytes (Fig. 1B) or the vehicle (PBS) were injected i.v. into the chronic colitis model after transfer of CD4⁺ MLN T cells from SAMP1 mice (Fig. 1A), then changes in several inflammatory parameters were evaluated. The inflammatory parameters BW loss (Fig. 1C), colon shortening (Fig. 1D and E), and histological scores for the large intestine (Fig. 1F and G) showed similar levels of severity in the chronic colitis mice following transfer of ACs or PBS. In addition, the expression levels of pro-inflammatory cytokines, IL-1 β , and MIP-2 were similar between the AC and PBS groups (Fig. 1H).

ACs adoptively co-transferred with CD19⁺ B cells ameliorate intestinal inflammation in chronic colitis mice

We next investigated the effects of ACs in the presence of co-transferred CD19⁺ splenocytes on chronic intestinal inflammation. ACs or the vehicle (PBS) were injected i.v. into the chronic colitis model after transfer of CD19⁺ splenocytes from AKR mice and CD4⁺ MLN T cells from SAMP1 mice (Fig. 2A), then changes in several inflammatory parameters in both groups were evaluated. The inflammatory parameters BW loss (Fig. 2B), colon shortening (Fig. 2C and D), and histological scores for the large intestine in chronic colitis mice were significantly less severe in the AC group as

compared to those in the PBS group (Fig. 2E and F). In addition, the expression levels of IL-1 β and MIP-2 were also significantly lower in the AC group (Fig. 2G).

Co-transfer with CD19^{hi}CD1d^{hi}-depleted B cells tends to deteriorate intestinal inflammation

We further investigated whether the effects of ACs on chronic intestinal inflammation are dependent on the sub-population of regulatory B cells. Recently, we reported that CD19^{hi}CD1d^{hi} B cells produce high levels of IL-10 and were considered to be a Bregs population (22). Consequently, a CD19^{hi}CD1d^{hi}-depleted B cell population can be considered to be a Breg-depleted B cell population. ACs or the vehicle (PBS) were injected i.v. into the chronic colitis model after transfer of CD19^{hi}CD1d^{hi}-depleted B cells from AKR mice and CD4⁺ MLN T cells from SAMP1 mice (Fig 3A and B), then changes in several inflammatory parameters in both groups were evaluated. The inflammatory parameters BW loss (Fig. 3C), colon shortening (Fig. 3D and E), and histological scores for the large intestine (Fig. 3F and G) in the chronic colitis mice were slightly more severe in the AC group as compared to those in PBS group, though the difference was not significant. Also, the expression levels of IL-1 β and MIP-2 were slightly higher in the AC group, though again the difference was not significant (Fig. 3H).

ACs induce IL-10 production in splenic B cells

To investigate possible interaction between ACs and B cells, we injected Dex-induced syngeneic apoptotic thymocytes (Fig. 1B) or the vehicle alone (PBS) into AKR mice. Three weeks later, CD19⁺ splenocytes from both groups were cultured in the presence

or absence of PMA and ionomycin. IL-10-producing B cells were found in the AC group at increased frequency as compared to the PBS group under both stimulated and un-stimulated conditions (Fig. 4A). Furthermore, B cells from the AC group produced a significantly higher level of IL-10 as compared to those from the PBS group under both conditions (Fig. 4B).

Phagocytosis of ACs a prerequisite to induce splenic B cells

We then examined whether ACs interact directly with splenic B cells to induce IL-10 production or indirectly exert their effects after undergoing phagocytosis. For this purpose, we selected MFG-E8 KO mice, which are characterized by impaired uptake of apoptotic cells (23), as the host strain. Syngeneic ACs or the vehicle (PBS) were injected into MFG-E8 KO mice. Three weeks later, CD19⁺ splenocytes from both groups were cultured in the presence or absence of PMA and ionomycin. Although IL-10 production from B cells were similar in both the AC and PBS groups under the stimulated condition, those from the AC group produced significantly lower levels of IL-10 as compared to B cells from the PBS group under the un-stimulated condition (Fig. 4C).

Apoptosis induced by reactive oxygen species (ROS) in circulating neutrophils during GMA

GMA is used as a therapeutic option for induction therapy for several immune-mediated disorders including IBD, rheumatoid arthritis (RA) and psoriasis (33-35). An Adacolumn is an adsorptive type carrier-based medical device for GMA and its major components are cellulose acetate beads, which absorb activated granulocytes and

monocytes from peripheral blood. The main concept behind the development of the Adacolumn is removal of activated leukocytes for preventing their migration to inflammatory sites. However, the actions of the column are more than just removing leukocytes, as a type of immunomodulation has also been suggested by results of several clinical or basic research studies (36-38). ROS are generated in the Adacolumn by contact between the beads and activated leukocytes, which change the leukocyte cell surface markers to L-selectin^{low} (26, 39). Previous studies have shown that apoptosis develops in leukocytes characterized by those markers (40). Thus, we speculated that a considerable number of apoptotic leukocytes induced by ROS in the Adacolumn re-enter the body and contribute to the efficacy of GMA.

We used a rabbit immune arthritis model for investigating ROS-induced apoptosis of circulating neutrophils during GMA (Fig. 5A). Photon counts were gradually increased after initiation of GMA, which was not found in a sham apheresis model (Fig. 5B). Furthermore, generation of O₂⁻ in the column was confirmed by infusion of superoxide dismutase into the column. Thereafter, photon counts were reduced to the baseline level (data not shown). Also, a significant decrease in L-selectin expression on neutrophils was observed in the GMA outflow (Fig. 5C), while hypodiploid apoptotic neutrophils were also significantly increased in the outflow (Fig. 5D and E). These results suggest that apoptosis is induced by ROS in circulating neutrophils during GMA and a considerable number of apoptotic neutrophils re-enter the body.

H₂O₂-induced apoptotic neutrophils ameliorate mice colitis

We selected mice colitis model to reveal immunomodulatory effect of apoptotic

neutrophils generated during GMA therapy. To mimic apoptotic neutrophils generated during GMA therapy, we isolated PECs, containing 65% to 85% neutrophils (31), from AKR mice and induced them to undergo apoptosis by exposure to H₂O₂, one kind of ROS. That treatment changed the neutrophil surface marker to L-selectin^{low}, which was similar to the change found in cells after contact with the Adacolumn beads (Fig. 6A). In addition, we confirmed apoptosis induction in those cells by Annexin-V staining (Fig. 6B). Next, we replaced the apoptotic thymocytes with apoptotic PECs (APECs) and investigated the anti-inflammatory effects of i.v. injection of APECs in the SCID chronic colitis model in the presence of co-transferred CD19⁺ splenocytes (Fig. 6C). The inflammatory parameters BW loss (Fig. 6D), histological scores for the large intestine (Fig. 6E and F), and expression levels of pro-inflammatory cytokines in the colitis mice were less severe in the AC group as compared to the PBS group (Fig. 6G).

Discussion

In the present study, injection of ACs ameliorated chronic intestinal inflammation in mice only in the presence of co-transferred whole B cells and not in their absence. Furthermore, the ameliorative effect of ACs was lost when whole B cells were replaced by IL-10-producing CD19^{hi}CD1d^{hi}-depleted B cells. In addition, injection of ACs induced IL-10 production in host splenic B cells only in the presence of normal phagocytic function. These novel findings show that ACs have potential to activate the pre-existing Breg population into IL-10 secreting active mode and/or induce differentiation of immature B cells into Bregs. In addition, we showed the possibility that AC-mediated inhibition of colitis may be an anti-inflammatory mechanism of GMA for IBD.

Potent inducers of AC death such as ultraviolet irradiation and X-ray exposure ameliorate inflammatory diseases (45, 46), while sepsis-induced apoptosis suppresses delayed type hypersensitivity in mice (47). Recently, adoptively transferred ACs were reported to protect mice from autoimmune diseases, including collagen-induced arthritis (CIA) (11) and experimental autoimmune encephalitis (48). In addition, transfusion of donor ACs prolonged heart allograft survival in rats (49) and skin allograft survival in a mice model (50). According to those reports, ACs can exert their protective effect in a variety of immune-mediated disorders regardless of whether apoptosis was induced *in vivo* or ACs induced with an *in vitro* method were administered in an adoptive manner. Although the positive impact of ACs has been demonstrated in autoimmune inflammation and allograft survival enhancement, there is no report of the role of ACs in chronic intestinal inflammation.

In the present study, we investigated the effects of ACs in an adoptive transfer

model of mice colitis and found that their injection had no effects, positive or negative, on the severity of colitis in SCID mice. Previous studies have revealed that most CD4⁺ T cells isolated from SAMP1 mice are already activated (51). In addition, Tregs have been reported to be dysfunctional in SAMP1 mice (52). These findings might explain why ACs failed to reduce colitis severity in the present model.

Our recent findings showed that Bregs expressing IL-10 play an important role in the pathogenesis of ileitis in SAMP1 mice (53). Furthermore, co-transferred Breg-depleted B cells exacerbated colitis in SCID mice transferred with SAMP1 CD4⁺ T cells (22). The role of Bregs has also been shown in several colitis models such as TCR- α - and G α i2-deficient mice (54-56), and they are considered to contribute to immune modulation in the intestinal tract. Since SCID mice do not have mature B cells, we speculated that ACs may play an important role to reduce the severity of chronic colitis co-functioning with Bregs. The present results indicated that colitis activity was significantly lower in mice following co-transfer of whole CD19⁺ B cells and ACs as compared to that in colitis mice following co-transfer of whole CD19⁺ B cells and PBS. We recently reported that IL-10-producing Bregs were enriched in a population of CD19^{hi}CD1d^{hi} B cells (22). To further confirm the role of Bregs in the beneficial effects of ACs, we co-transferred CD19^{hi}CD1d^{hi}-depleted B cells and ACs to colitis mice. Our results indicated that depletion of Bregs canceled out the effect of ACs, suggesting that the anti-inflammatory activities of ACs are dependent on the presence of Bregs.

Several reports have shown that intravenous injection delivers ACs to the spleen (11, 57), while it is known that systemic tolerance to ACs is dependent on splenic function (58). Thus, we focused on the interaction of injected ACs with splenic B cells *in vivo*. Our results demonstrated an increased frequency of IL-10-producing B cells in

AC-injected mice as compared to that of PBS-injected mice in both the presence and absence of stimulation. Furthermore, splenic CD19⁺ B cells from the AC group produced significantly higher levels of IL-10 as compared to those from the PBS group under basal and activated conditions. The present finding that AC-induced IL-10 production in splenic B cells *in vivo* is consistent with other recent findings (11, 48). Gray M. *et al.* reported that inhibition of IL-10 *in vivo* reversed the beneficial effect of ACs in collagen-induced arthritis (CIA) (11), while CIA was reported to exacerbate in IL-10-deficient mice (59, 60). IL-10 is a multifunctional cytokine with an ability to inhibit activation and effector functions of various immune cells (61). However, it remains unknown whether the anti-inflammatory effects of ACs are simply dependent on IL-10 production by Bregs. The mechanisms by which regulatory function can be imparted to B cells by interaction with ACs require further investigation.

We also investigated whether injected ACs interacted directly or indirectly with splenic B cells after engulfment by splenic phagocytes to induce IL-10 production. As the host strain, we employed MFG-E8 KO mice, which are characterized by impaired uptake of apoptotic cells (23). Our results indicated that splenic CD19⁺ B cells from both the AC and PBS groups produced similar levels of IL-10 in both the presence and absence of stimulation. This novel finding demonstrated that phagocytosis of ACs is a prerequisite for induction of IL-10-producing B cells. Ravishankar *et al.* (50) reported that AC-mediated allograft tolerance requires CD169⁺ macrophages located in the splenic marginal zone. Deficiency in removal of ACs can lead to autoimmune disorders such as SLE (8, 62). AC-induced tolerance in allogeneic heart transplants was reported to be prevented by administrations of gadolinium chloride, which disrupts phagocyte function, and annexin V, which blocks the binding of exposed phosphatidylserine to its

receptor on phagocytes (49). Thus, without being phagocytosed, ACs are unable to induce immune tolerance. We speculated that phagocytosis of injected ACs plays a decisive role in influencing generation of IL-10-producing Bregs, which in turn determines the outcome of adoptively transferred colitis. Recent studies have revealed that IL-10 production by B cells *in vitro* requires direct contact with ACs (11, 48). Additional studies of the direct interactions between ACs and B cells *in vivo* are necessary to clarify this point.

GMA, a type of cytapheresis, is used as induction therapy for IBD in Japan and European countries (41-43). Its efficacy is dependent on removing circulating activated leukocytes with an Adacolumn device, which prevents their migration to inflammatory sites in the intestine. Post-marketing surveillance in Japan of 697 UC patients treated at 53 medical institutions over 7 years from 1999 to 2006 was undertaken by the manufacturer, which showed satisfactory clinical efficacy and safety (41). Although the efficacy of GMA is similar to that of other leukocytapheresis methods, the average adsorption rate of leukocytes to an Adacolumn is relatively low (30-40%) as compared to other methods. Thus, we considered that a considerable number of leukocytes re-enter the body after contact with the Adacolumn beads, which may be related to the anti-inflammatory effects of GMA. Experimental results have also revealed that ROS generated in the Adacolumn change the leukocyte cell surface markers to L-selectin^{low} and induce those cells to undergo apoptosis. Inbred strains of mice including, AKR, are deficient in components of complement (44), while deposition of complement fragments, such as C3bi, as ligand for CR3 onto Adacolumn beads is one of the requirements for effective removal of activated leukocytes (27). Thus, we could not use mice apoptotic leukocytes induced by the Adacolumn beads. In the present study, we

examined the effects of injected H₂O₂-induced apoptotic leukocytes in an SCID colitis model co-transferred with whole B cells and found that injection of APECs reduced colitis severity, suggesting that apoptotic leukocytes induced by ROS generated in the Adacolumn may contribute to the efficacy of GMA. To confirm the anti-inflammatory mechanisms of GMA associated with induction and efficacy of ACs, additional experiments are required.

In the present study, we demonstrated that injection of ACs reduced the severity of mice colitis in the presence of IL-10-producing CD19^{hi}CD1d^{hi} B cells. We also speculate that this ameliorative effect of ACs might be one of the anti-inflammatory mechanisms of GMA for IBD. However, it remains unknown whether ACs activate pre-existing Bregs or cause immature B cells to differentiate into Bregs. Elucidation of the detailed mechanisms of AC-mediated anti-inflammatory effects may lead to a novel therapeutic strategy for IBD.

References

1. Vaux DL. Toward an understanding of the molecular mechanisms of physiological cell death. *Proc Natl Acad Sci USA*. 1993;90:786-789.
2. Savill J, Fadok V, Henson P, et al. Phagocyte recognition of cells undergoing apoptosis. *Immunol Today*. 1993;14:131-136.
3. Ferguson TA, Stuart PM, Herndon JM, et al. Apoptosis, tolerance, and regulatory T cells--old wine, new wineskins. *Immunol Rev*. 2003;193:111-123.
4. Green DR, Ferguson T, Zitvogel L, et al. Immunogenic and tolerogenic cell death. *Nat Rev Immunol*. 2009;9:353-363.
5. Griffith TS, Kazama H, VanOosten RL, et al. Apoptotic cells induce tolerance by generating helpless CD8⁺T cells that produce TRAIL. *J Immunol*. 2007;178:2679-2687.
6. Ferguson TA, Herndon J, Elzey B, et al. Uptake of apoptotic antigen-coupled cells by lymphoid dendritic cells and cross-priming of CD8(+) T cells produce active immune unresponsiveness. *J Immunol*. 2002;168:5589-5595.
7. Steinman RM, Turley S, Mellman I, et al. The induction of tolerance by dendritic cells that have captured apoptotic cells. *J Exp Med*. 2000;191:411-416.
8. Bijl M, Reefman E, Horst G, et al. Reduced uptake of apoptotic cells by macrophages in systemic lupus erythematosus: correlates with decreased serum levels of complement. *Ann Rheum Dis*. 2006;65:57-63.
9. Fadok VA, Bratton DL, Konowal A, et al. Macrophages that have ingested apoptotic cells in vitro inhibit proinflammatory cytokine production through autocrine/paracrine mechanisms involving TGF-beta, PGE2, and PAF. *J Clin Invest*. 1998;101:890-898.

10. Liu K, Iyoda T, Saternus M, et al. Immune tolerance after delivery of dying cells to dendritic cells in situ. *J Exp Med.* 2002;196:1091-1097.
11. Gray M, Miles K, Salter D, et al. Apoptotic cells protect mice from autoimmune inflammation by the induction of regulatory B cells. *Proc Natl Acad Sci USA.* 2007;104:14080-14085.
12. Notley CA, Brown MA, Wright GP, et al. Natural IgM is required for suppression of inflammatory arthritis by apoptotic cells. *J Immunol.* 2011;186:4967-4972.
13. Chen Y, Khanna S, Goodyear CS, et al. Regulation of dendritic cells and macrophages by an anti-apoptotic cell natural antibody that suppresses TLR responses and inhibits inflammatory arthritis. *J Immunol.* 2009;183:1346-1359.
14. Voll RE, Herrmann M, Roth EA, et al. Immunosuppressive effects of apoptotic cells. *Nature.* 1997;390:350-351.
15. Marteau P. Inflammatory bowel disease. *Endoscopy.* 2000;32:131-137.
16. Podolsky DK. Inflammatory bowel disease. *N Engl J Med.* 1991;325:928-937.
17. Satsangi J, Jewell D, Parkes M, et al. Genetics of inflammatory bowel disease. A personal view on progress and prospects. *Dig Dis.* 1998;16:370-374.
18. Satsangi J, Welsh KI, Bunce M, et al. Contribution of genes of the major histocompatibility complex to susceptibility and disease phenotype in inflammatory bowel disease. *Lancet.* 1996;347:1212-1217.
19. Duerr RH. Genetics of inflammatory bowel disease. *Inflamm Bowel Dis.* 1996;2:48-60.
20. Papadakis KA, Targan SR. Current theories on the causes of inflammatory bowel disease. *Gastroenterol Clin North Am.* 1999;28:283-296.

21. Noguchi M, Hiwatashi N, Liu Z, et al. Secretion imbalance between tumour necrosis factor and its inhibitor in inflammatory bowel disease. *Gut*.1998;43:203-209.
22. Oka A, Ishihara S, Mishima Y et al. Role of regulatory B cells in chronic intestinal inflammation: association with pathogenesis of Crohn's disease. *Inflamm Bowel Dis*. 2014;20:315-328.
23. Hanayama R, Tanaka M, Miyasaka K, et al. Autoimmune disease and impaired uptake of apoptotic cells in MFG-E8-deficient mice. *Science*. 2004;304:1147-1150.
24. Burns RC, Rivera-Nieves J, Moskaluk CA, et al. Antibody blockade of ICAM-1 and VCAM-1 ameliorates inflammation in the SAMP-1/Yit adoptive transfer model of Crohn's disease in mice. *Gastroenterology*. 2001;121:1428-1436.
25. Pettipher EA, Henderson B, Moncada S, et al. Leucocyte infiltration and cartilage proteoglycan loss in immune arthritis in the rabbit. *Br. J. Pharmacol*. 1988;98:176-196.
26. Kashiwagi N, Nakano M, Saniabadi AR, et al. Anti-inflammatory effect of granulocyte and monocyte adsorption apheresis in a rabbit model of immune arthritis. *Inflammation*. 2002;26:199-205.
27. Takeda Y, Shiobara N, Saniabadi AR, et al. Adhesion dependent release of hepatocyte growth factor and interleukin-1 receptor antagonist from human granulocytes and monocytes: Evidence for the involvement of plasma IgG, complement C3 and b2 integrin. *Inflamm res*. 2004;53:277-283.
28. Uehara K, Maruyama N, Huang C, et al. The first application of a chemiluminescence probe for detecting O₂-production in vitro from Kupffer cells stimulated by phorbol myristate acetate. *FEBS*. 1993;335:167-170.

29. Roberts RL, Gallin JI. Rapid method for isolation of normal human peripheral blood eosinophils on discontinuous Percoll gradients and comparison with neutrophils. *Blood*. 1985;65:433-440.
30. Dransfield I, Buckle AM, Savill JS, et al. Neutrophil apoptosis is associated with a reduction in CD16 (FcγRIII) expression. *J Immunol*. 1994;153:1254-1263.
31. Kannan Y, Ushio H, Koyama H, et al. 2.5S nerve growth factor enhances survival, phagocytosis, and superoxide production of murine neutrophils. *Blood*. 1991;77:1320-1325.
32. Kannan Y, Usami K, Okada M, et al. Nerve growth factor suppresses apoptosis of murine neutrophils. *Biochem. Biophys. Res. Commun*. 1992;186:1050-1056.
33. Sacco R, Romano A, Mazzoni A, et al. Granulocytapheresis in steroid-dependent and steroid-resistant patients with inflammatory bowel disease: a prospective observational study. *J Crohns Colitis*. 2013;7:e692-697.
34. Fukuchi T, Nakase H, Matsuura M, et al. Effect of intensive granulocyte and monocyte adsorptive apheresis in patients with ulcerative colitis positive for cytomegalovirus. *J Crohns Colitis*. 2013;7:803-811.
35. Ikeda S, Takahashi H, Suga Y, et al. Therapeutic depletion of myeloid lineage leukocytes in patients with generalized pustular psoriasis indicates a major role for neutrophils in the immunopathogenesis of psoriasis. *J Am Acad Dermatol*. 2013;68:609-617.
36. Diepolder HM, Kashiwagi N, Teuber G, et al. Leucocytapheresis with Adacolumn enhances HCV-specific proliferative responses in patients infected with hepatitis C virus genotype 1. *J Med Virol*. 2005;77:209-215.
37. Noguchi A, Watanabe K, Narumi S, et al. The production of

- interferon-gamma-inducible protein 10 by granulocytes and monocytes is associated with ulcerative colitis disease activity. *J Gastroenterol.* 2007;42:947-956.
38. Kashiwagi N, Hirata I, Kasukawa R. A role for granulocyte and monocyte apheresis in the treatment of rheumatoid arthritis. *Ther Apher.* 1998;2:134-141.
39. Ramlow W, Emmrich J, Ahrenholz P, et al. In vitro and in vivo evaluation of Adacolumn cytapheresis in healthy subjects. *J Clin Apher.* 2005;20:72-80.
40. Dransfield I, Stocks SC, Haslett C. Regulation of cell adhesion molecule expression and function associated with neutrophil apoptosis. *Blood.* 1995;85:3264-3273.
41. Hibi T1, Sameshima Y, Sekiguchi Y, et al. Treating ulcerative colitis by Adacolumn therapeutic leucocytapheresis: clinical efficacy and safety based on surveillance of 656 patients in 53 centres in Japan. *Dig Liver Dis.* 2009;41:570-577.
42. Vecchi M1, Vernia P, Riegler G, et al. Therapeutic landscape for ulcerative colitis: where is the Adacolumn® system and where should it be? *Clin Exp Gastroenterol.* 2013;6:1-7.
43. Linton L1, Karlsson M, Grundström J, et al. HLA-DR(hi) and CCR9 Define a Pro-Inflammatory Monocyte Subset in IBD. *Clin Transl Gastroenterol.* 2012;3:e29.
44. Wetsel RA, Fleischer DT, Haviland DL. Deficiency of the murine fifth complement component (C5). *J. Biol. Chem.* 1990;265:2435-2440.
45. Abel EA. Phototherapy. *Dermatol Clin.* 1995;13:841-849.
46. Trott KR. Therapeutic effects of low radiation doses. *Strahlenther Onkol.* 1994;170:1-12.
47. Unsinger J, Kazama H, McDonough JS, et al. Sepsis-induced apoptosis leads to active suppression of delayed-type hypersensitivity by CD8+ regulatory T cells through a TRAIL-dependent mechanism. *J Immunol.* 2010;184:6766-6772.

48. Miles K, Heaney J, Sibinska Z, et al. A tolerogenic role for Toll-like receptor 9 is revealed by B-cell interaction with DNA complexes expressed on apoptotic cells. *Proc Natl Acad Sci USA*. 2012;109:887-892.
49. Sun E, Gao Y, Chen J, et al. Allograft tolerance induced by donor apoptotic lymphocytes requires phagocytosis in the recipient. *Cell Death Differ*. 2004;11:1258-1264.
50. Ravishankar B, Shinde R, Liu H, et al. Marginal zone CD169⁺ macrophages coordinate apoptotic cell-driven cellular recruitment and tolerance. *Proc Natl Acad Sci USA*. 2014;111:4215-4220.
51. Kosiewicz MM, Nast CC, Krishnan A, et al. Th1-type responses mediate spontaneous ileitis in a novel murine model of Crohn's disease. *J Clin Invest*. 2001;107:695-702.
52. Ishikawa D, Okazawa A, Corridoni D, et al. Tregs are dysfunctional in vivo in a spontaneous murine model of Crohn's disease. *Mucosal Immunol*. 2013;6:267-275.
53. Mishima Y, Ishihara S, Aziz MM, et al. Decreased production of interleukin-10 and transforming growth factor- β in Toll-like receptor-activated intestinal B cells in SAMP1/Yit mice. *Immunology*. 2010;131:473-487.
54. Mizoguchi A, Mizoguchi E, Smith RN, et al. Suppressive role of B cells in chronic colitis of T cell receptor alpha mutant mice. *J Exp Med*. 1997;186:1749-1756.
55. Wei B, Velazquez P, Turovskaya O, et al. Mesenteric B cells centrally inhibit CD4⁺T cell colitis through interaction with regulatory T cell subsets. *Proc Natl Acad Sci USA*. 2005;102:2010-2015.
56. Brummel R, Lenert P. Activation of marginal zone B cells from lupus mice with type A(D) CpG-oligodeoxynucleotides. *J Immunol*. 2005;174:2429-2434.

57. Morelli AE, Larregina AT, Shufesky WJ, et al. Internalization of circulating apoptotic cells by splenic marginal zone dendritic cells: dependence on complement receptors and effect on cytokine production. *Blood*. 2003;101:611-620.
58. Streilein JW, Niederkorn JY. Induction of anterior chamber-associated immune deviation requires an intact, functional spleen. *J Exp Med*. 1981;153:1058-1067.
59. Finnegan A, Kaplan CD, Cao Y, et al. Collagen-induced arthritis is exacerbated in IL-10-deficient mice. *Arthritis Res Ther*. 2003;5:R18-24.
60. Johansson AC, Hansson AS, Nandakumar KS, et al. IL-10-deficient B10.Q mice develop more severe collagen-induced arthritis, but are protected from arthritis induced with anti-type II collagen antibodies. *J Immunol*. 2001;167:3505-3512.
61. Moore KW, de Waal Malefyt R, Coffman RL, et al. Interleukin-10 and the interleukin-10 receptor. *Annu Rev Immunol*. 2001;19:683-765.
62. Ginaldi L, Martinis MD, D'Ostilio A, et al. Cell proliferation and apoptosis in the immune system in the elderly. *Immunol. Res*. 2000;21:31-38.

Figure legends

Figure 1

ACs alone did not ameliorate intestinal inflammation in SAMP1 CD4⁺ MLN T cell-induced chronic colitis mice. (A) Protocol for induction of SAMP1 CD4⁺ MLN T cell-mediated chronic colitis in SCID mice and AC injection. Purified CD4⁺ T cells (5×10^5 cells/mouse) derived from MLN cells of SAMP1 mice were injected intraperitoneally on day 1 into 8-10 week old SCID mice. (B) Dex-treated thymocytes were subjected to flow cytometry after staining with annexin V and 7-AAD. (C) Effects of ACs on BW changes in SAMP1 CD4⁺ MLN T cell-induced chronic colitis. The AC group (squares) was given an i.v. injection of ACs (1×10^7 cells/mouse) on week 1, whereas the control group received the vehicle alone (triangle). Data are expressed as serial changes in percentage of weight change over a 7-week period. Error bars indicate SEM values obtained from mice in each group (n=5). (D) Representative images of colons dissected from mice in each experimental group. (E) Effects of ACs on colon length in SAMP1 CD4⁺ MLN T cell-induced chronic colitis. Error bars indicate SEM values obtained from mice in each group (n=5). (F) Representative images of histological changes in large intestines at 7 weeks after SAMP1 CD4⁺ MLN T cell injection with or without ACs. (G) Mean values of intestinal histological scores in each experimental group. Error bars indicate SEM values obtained from mice in each group (n=5). (H) Gene expressions of IL-1 β and MIP-2 in large intestines in each experimental group. Error bars indicate SEM values obtained from mice in each group (n=5).

Figure 2

ACs ameliorated intestinal inflammation in SAMP1 CD4⁺ MLN T cell-induced chronic colitis mice when co-transferred with CD19⁺ splenocytes. (A) Protocol for co-transfer of CD19⁺ splenocytes and ACs in SAMP1 CD4⁺ MLN T cell-induced chronic colitic SCID mice. Purified whole CD19⁺ splenocytes (2×10^6 cells/mouse) derived from AKR mice and SAMP1 CD4⁺ MLN T cells (5×10^5 cells/mouse) were injected i.v. on day 0 and intraperitoneally on day 1, respectively, into 8-10 week old SCID mice. (B) Effects of ACs on BW changes in CD19⁺ splenocytes injected into SAMP1 CD4⁺ MLN T cell-induced chronic colitic mice. The AC group (squares) were given an i.v. injection of ACs (1×10^7 cells/mouse) on week 1, whereas the control group received the vehicle alone (triangle). Data are expressed as serial changes in percentage of weight change over a 7-week period. Error bars indicate SEM values obtained from mice in each group (n= 9) (* $p < 0.04$ and # $p < 0.01$ vs. PBS). (C) Representative images of colons dissected from mice in each experimental group. (D) Effects of ACs on colon length in CD19⁺ splenocytes injected into SAMP1 CD4⁺ MLN T cell-induced chronic colitic mice. Error bars indicate SEM values obtained from mice in each group (n=9) (* $p < 0.02$ vs. PBS). (E) Representative images of histological changes in large intestines at 7 weeks after injection of CD19⁺ splenocytes and SAMP1 CD4⁺ MLN T cells with or without ACs. (F) Mean values of intestinal histological scores in each experimental group. Error bars indicate SEM values obtained from mice in each group (n=9) (* $p < 0.01$ vs. PBS). (G) Gene expressions of IL-1 β and MIP-2 in large intestines in each experimental group. Error bars indicate SEM values obtained from mice in each group (n=9) (* $p < 0.001$ and # $p < 0.02$ vs. PBS).

Figure 3

AC-mediated ameliorative effects were lost in the absence of the sub-population of Bregs. (A) Protocol for co-transfer of Bregs-depleted CD19⁺ splenocytes and ACs in SAMP1 CD4⁺ MLN T cell-induced chronic colitic SCID mice. Flow cytometry-sorted CD19^{hi}CD1d^{hi}-depleted B cells (2×10^6 cells/mouse) derived from AKR mice and SAMP1 CD4⁺ MLN T cells (5×10^5 cells/mouse) were injected i.v. on day 0 and intraperitoneally on day 1, respectively, into 8-10 week old SCID mice. (B) CD19^{hi}CD1d^{hi}-depleted B cells were sorted by flow cytometry from CD19⁺ splenocytes derived from 15-25 week old AKR mice. (C) Effects of ACs on BW changes following injection of CD19^{hi}CD1d^{hi}-depleted B cells into SAMP1 CD4⁺ MLN T cell-induced chronic colitic mice. The AC group (squares) was given an i.v. injection of ACs (1×10^7 cells/mouse) on week 1, whereas the control group received the vehicle alone (triangle). Data are expressed as serial changes in percentage of weight change over a 6-week period. Error bars indicate SEM values obtained from mice in each group (n=4). (D) Representative images of colons dissected from mice in each experimental group. (E) Effects of ACs on colon length following injection of CD19^{hi}CD1d^{hi}-depleted B cells into SAMP1 CD4⁺ MLN T cell-induced chronic colitic mice. Error bars indicate SEM values obtained from mice in each group (n=4). (F) Representative images of histological changes in large intestines at 6 weeks after injection of CD19^{hi}CD1d^{hi}-depleted B cells and SAMP1 CD4⁺ MLN T cells with or without ACs. (G) Mean values of intestinal histological scores in each experimental group. Error bars indicate SEM values obtained from mice in each group (n=4). (H) Gene expressions of IL-1 β and MIP-2 in large intestines in each experimental group. Error bars indicate SEM values obtained from mice in each group (n=4).

Figure 4

ACs induced IL-10 production in splenic B cells only in the presence of normal phagocytic function. (A) Effects of AC injection on the number of splenic B cells expressing IL-10 in AKR mice. The AC group was given an i.v. injection of syngeneic ACs (1×10^7 cells/mouse), whereas the control group received the vehicle (PBS) alone. Three weeks later, CD19⁺ splenocytes were harvested from both groups, and cultured for 72 hours in the presence or absence of PMA and ionomycin. The expressions of CD19 and IL-10 were examined by flow cytometry. Representative dot plots showing expressions of CD19 and IL-10 in B cells are presented. (B) Effects of AC injection on production of IL-10 by splenic B cells in AKR mice. The AC group (blocked column) were given an i.v. injection of syngeneic ACs (1×10^7 cells/mouse), whereas the control group received the vehicle (PBS) alone (open column). Three weeks later, CD19⁺ splenocytes were harvested from both groups and cultured for 72 hours in the presence or absence of PMA and ionomycin, then supernatants were collected and IL-10 production was measured by ELISA. Error bars indicate SEM values obtained from mice in each group (n=3) (* $p < 0.001$ and # $p < 0.002$ vs. PBS). (C) Effects of AC injection on production of IL-10 by splenic B cells in MFG-E8 knockout mice. The AC group (blocked column) was given an i.v. injection of syngeneic ACs (1×10^7 cells/mouse), whereas the control group received the vehicle (PBS) alone (open column). Three weeks later, CD19⁺ splenocytes were harvested from both groups and cultured for 72 hours in the presence or absence of PMA and ionomycin, then supernatants were collected and IL-10 production was measured by ELISA. Error bars indicate SEM values obtained from mice in each group (n=3) (* $p < 0.02$ vs. PBS).

Figure 5

Superoxide anion radical produced in the GMA column, and shedding of L-selectin and enhancement of apoptosis in neutrophils from GMA column outflow. (A) GMA in rabbits with arthritis using a mini GMA column. (B) Each rabbit was continuously infused with 185 μM of MCLA at a flow rate of 10 ml/hour starting at 10 minutes prior to initiation of GMA (closed circle, n=4) or as sham (open circle, n=4) apheresis. The columns were placed inside the chamber of a photon counting unit shielded from light and apheresis was performed. The amount of the superoxide anion radical O_2^- was measured by directly counting the number of photons emitted by MCLA upon reaction with O_2^- . Error bars indicate SEM values obtained from mice in each group. (C) EDTA-blood samples from column inflow and outflow were labeled with an FITC conjugated anti-L-selectin monoclonal antibody (LAM1-3). Closed circle: GMA (n=11) (* p <0.0001 vs. Inflow); open circle: sham (n=11). Error bars indicate SEM values obtained from mice in each group. Inflow and outflow were compared using a Wilcoxon-signed-rank test. (D) A rabbit experimental arthritis model received GMA treatment. One hour after initiation of GMA, blood was collected from the GMA column inflow and outflow to isolate neutrophils. Cytometric analyses of PI-stained neutrophil nuclei were conducted after 18 hours of *in vitro* culture. Each overlay histogram shown is representative of 3 experiments. The proportion of apoptotic neutrophils was analyzed by gating on a broad hypodiploid peak. (E) Geometric mean PI fluorescence intensity of the hypodiploid peak from neutrophils in the inflow and outflow from the GMA column were compared using a paired t-test (n=3) (* p <0.02 vs. Inflow). Error bars indicate SEM values obtained from mice in each group.

Figure 6

APECs ameliorated intestinal inflammation in SAMP1 CD4⁺ MLN T cell-induced chronic colitic mice when co-transferred with CD19⁺ splenocytes. (A) Flow cytometric analysis of L-selectin expression on H₂O₂-treated or untreated PECs from AKR mice. PEC suspensions were treated with lysing solution to remove RBCs. PECs (2×10^6 cells/ml) were treated with 500 μ M H₂O₂ for 1 hour at 37°C, then stained with anti-CD62L MoAb for flow cytometric analysis. (B) H₂O₂-treated PECs were subjected to flow cytometry after staining with annexin V and 7-AAD. (C) Protocol for co-transfer of CD19⁺ splenocytes and APECs in SAMP1 CD4⁺ MLN T cell-induced chronic colitic SCID mice. Purified whole CD19⁺ splenocytes (2×10^6 cells/mouse) derived from AKR mice and SAMP1 CD4⁺ MLN T cells (5×10^5 cells/mouse) were injected i.v. on day 0 and intraperitoneally on day 1, respectively, into 8-10-week old SCID mice. (D) Effects of APECs on body weight changes following injection of CD19⁺ splenocytes into SAMP1 CD4⁺ MLN T cell-induced chronic colitic mice. The APEC group (squares) was given an i.v. injection of APECs (1×10^7 cells/mouse) on week 1, whereas the control group received the vehicle alone (triangle). Data are expressed as serial changes in percentage of weight change over a 7-week period. Error bars indicate SEM values obtained from mice in each group (n=5). (E) Representative images of histological changes in large intestines at 7 weeks after injection of CD19⁺ splenocytes and SAMP1 CD4⁺ MLN T cells with or without APECs. (F) Mean values of intestinal histological scores in each experimental group. Error bars indicate SEM values obtained from mice in each group (n=5) (* $p < 0.04$ vs. PBS). (G) Gene expressions of IL-1 β and MIP-2 in large intestines in each experimental group. Error bars indicate SEM values obtained from mice in each group (n=5) (* $p < 0.03$ vs. PBS).

List of Supplemental Digital Content

Supplemental Digital Content 1. .doc.

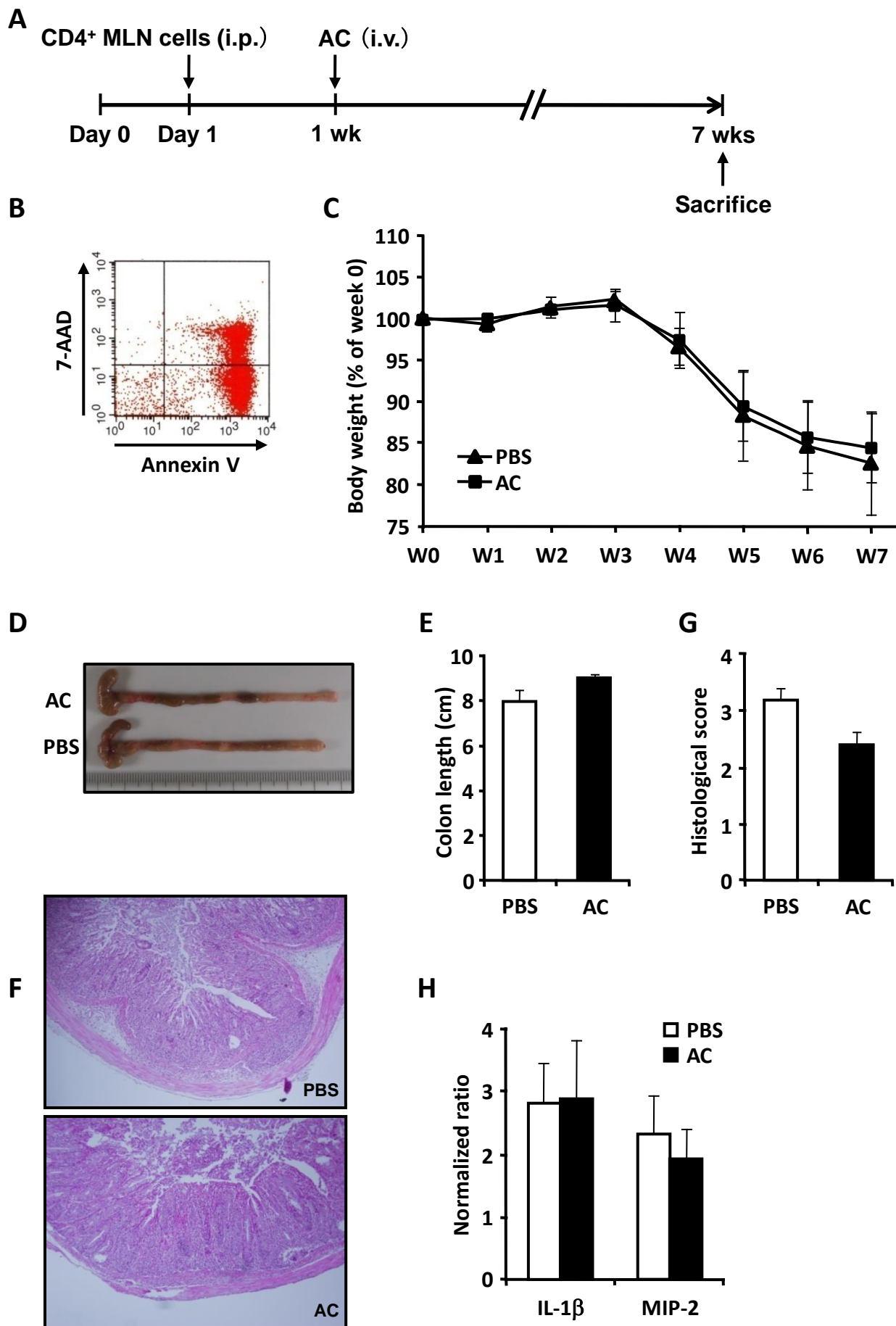
Table S1 shows the primer sequences for real-time PCR.

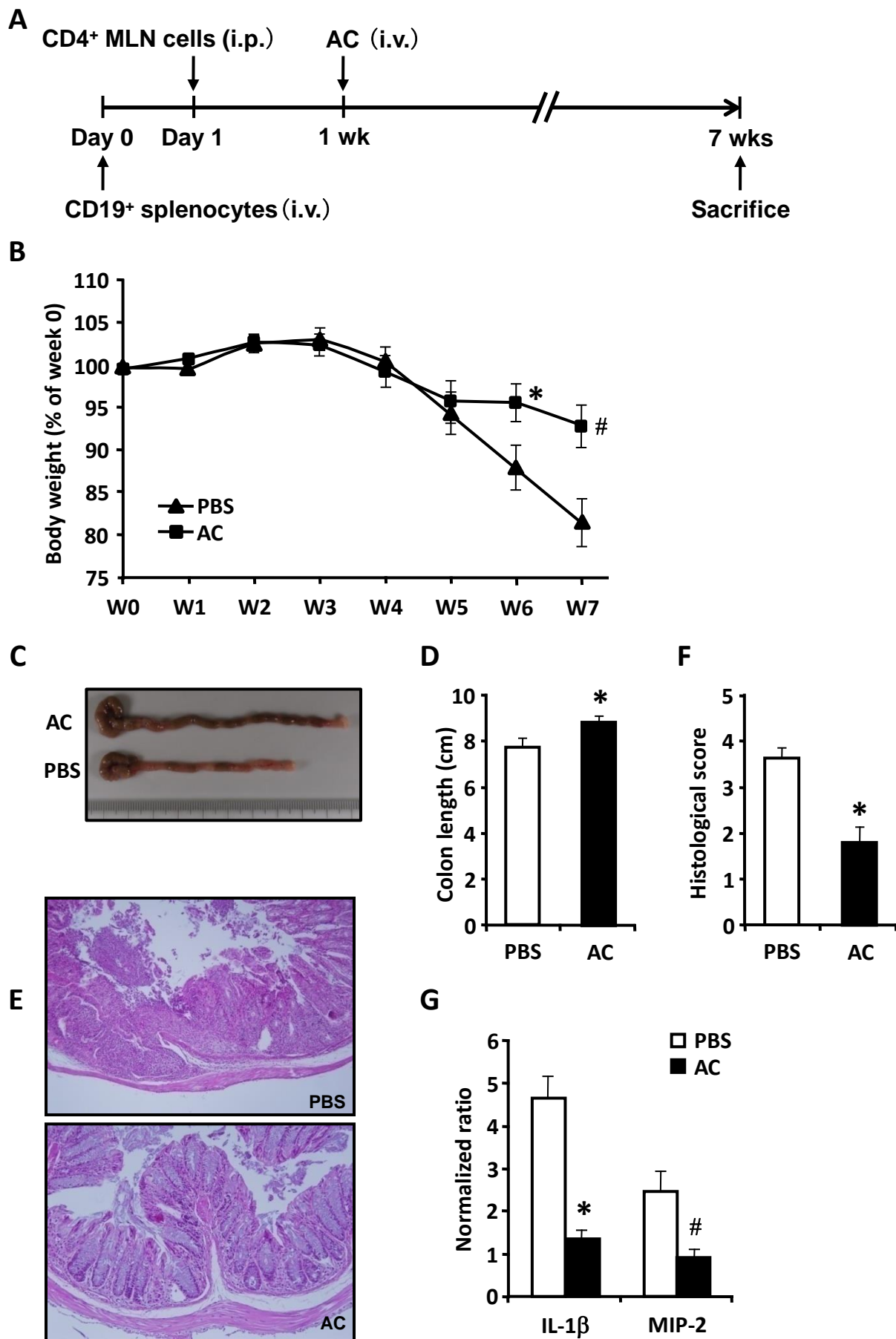
|

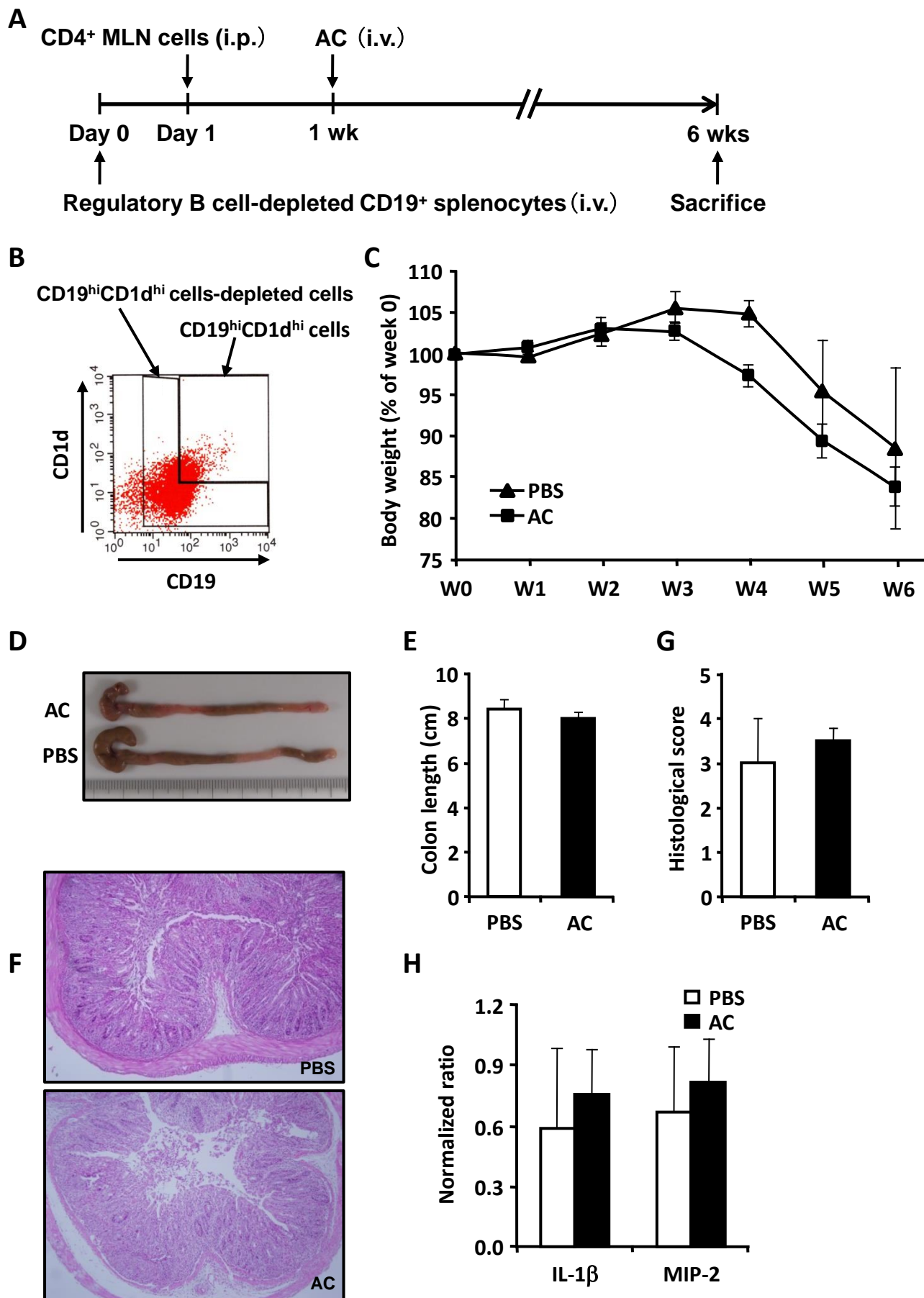
Table S1. Primer sequences for real-time PCR.

Gene (Accession No.)	Sequences (5'-3')
MIP-2 (NM_009140.2)	
Forward:	TCCAGAGCTTGAGTGTGACG
Reverse:	GCCCTTGAGAGTGGCTATGA
IL-1 β (NM_008361.3)	
Forward:	AGGCTCCGAGATGAACAACA
Reverse:	TTGGGATCCACACTCTCCA
β -Actin (NM_007393.3)	
Forward:	CACCAGTTCGCCATG GAT
Reverse:	CATCACACCCTGGTGCCTA

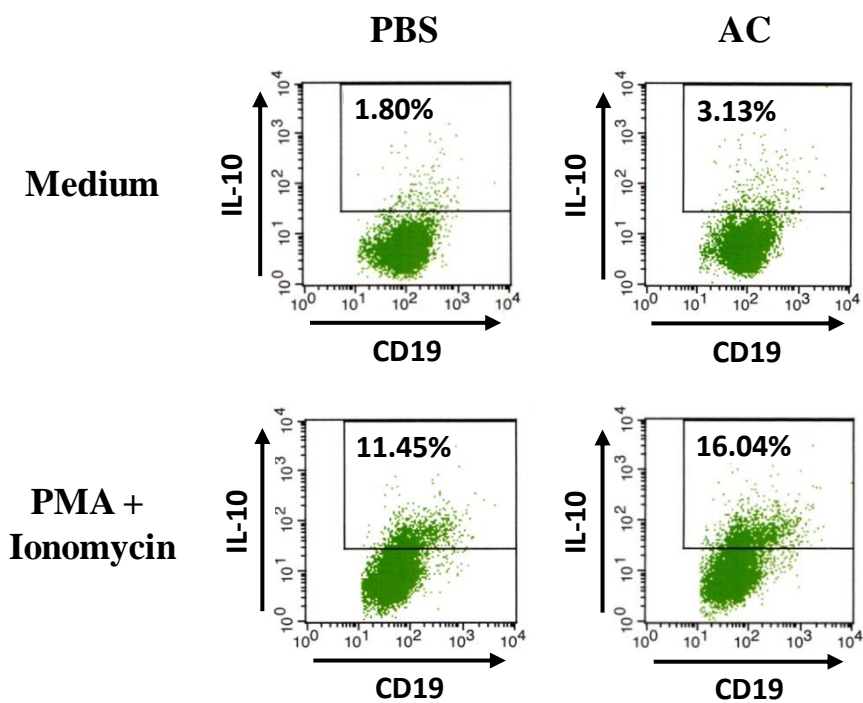
MIP, macrophage inflammatory protein; IL, interleukin;



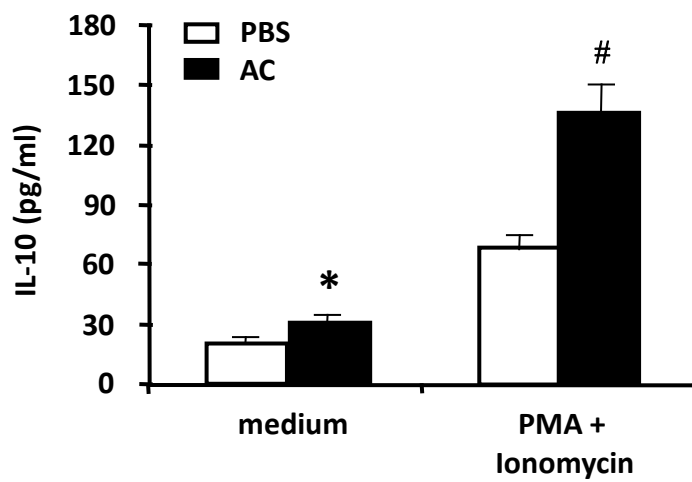




A



B



C

